Proceedings of the 43rd "Jaszowiec", International School and Conference on the Physics of Semiconductors, Wisła 2014

Structural and Optical Properties of Alternately-Strained ZnS_xSe_{1-x}/CdSe Superlattices with Effective Band-Gap 2.5–2.6 eV

E.A. Evropeytsev*, S.V. Sorokin, S.V. Gronin, I.V. Sedova, G.V. Klimko, A.A. Sitnikova, M.V. Baidakova, S.V. Ivanov and A.A. Toropov

Ioffe Physical-Technical Institute, Russian Academy of Sciences,
Politekhnicheskaya 26, 194021, St. Petersburg, Russia

We report on design and fabrication of alternately-strained ZnS_xSe_{1-x}/CdSe short period superlattices with the effective band-gap 2.52, 2.58, and 2.61 eV and the total thickness ≈ 300 nm. Transmission electron microscopy, X-ray diffraction, and photoluminescence measurements reveal negligibly small density of misfit dislocations in the superlattices. The investigation of carrier transport along the superlattice growth axis, performed by the photoluminescence measurements of a superlattice with one enlarged quantum well, confirms efficient Bloch-type transport at temperatures above ≈ 100 K. Such superlattices look promising for the applications as a material for the wide band-gap photoactive region of a multi-junction solar cell comprising both III–V and II–VI materials.

DOI: 10.12693/APhysPolA.126.1156

PACS: 78.67.Pt, 81.07.–b, 78.55.–m

1. Introduction

Integration of II–VI and III–V based cascades into a heterovalent multi-junction solar cell can make it possible to increase energy conversion efficiency in comparison with the solar cells based on III–V semiconductors alone [1]. The improvement is expected due to optimization of the captured spectrum of solar radiation as a result of using an additional wide band-gap II–VI cascade. High crystal quality of the II–VI cascade is needed to diminish recombination losses, which can be realized by pseudomorphic growth of the II–VI layers atop of the III–V cascade. Semiconductor alloys (Zn,Cd)(S,Se) look most suitable for the application as the II–VI cascade material because they have direct band-gap, can be lattice matched to GaAs, and can be doped by donor and acceptor dopants [2]. To obtain optimal band-gap energies of the II–VI cascade, corresponding to the maximum energy conversion efficiency of the heterovalent multijunction solar cell, it is important to be able to adjust band-gap of the (Zn,Cd)(S,Se) alloy flexibly within as wide energy range as possible, while maintaining low density of defects and efficient transport of photoexcited carriers. Technological control over the composition of the quaternary II–VI alloy is, however, a real challenge, whereas more realistic can be fabrication of an equivalent ZnS_xSe_{1-x} /CdSe short-period superlattice (SL).

In the present work we have designed and grown by molecular beam epitaxy (MBE) ZnS_xSe_{1-x} /CdSe pseudomorphic SLs with the effective band-gap energy E_g^{eff} in the range 2.5–2.6 eV (at 300 K) and investigated their structural and optical properties. The thicknesses and composition of the SL layers were calculated using a strain compensation concept based on the balance between tensile strain in ZnS_xSe_{1-x} layers and compressive strain in CdSe layers [3]. While designing the SL we also took into consideration that carrier mobility along the SL growth axis is defined by the corresponding lowest-energy miniband width. The width of a heavy-hole miniband is smaller than that of an electron one and, therefore, just this quantity limits the efficiency of the vertical transport of photoexcited carriers. To provide the efficient transport we have designed the SL with the heavy-hole miniband as wide as ≈ 50 meV. Investigation of the carrier vertical transport in the SL was performed by measurements of photoluminescence (PL) spectra of the structures containing the SL with one enlarged ZnSe/CdSe quantum well (QW) [4].

2. Experimental details

The structures were grown by MBE using a double-chamber setup (Semiteq, Russia) on undoped GaAs (001) substrates with epitaxial buffer layers of GaAs and ZnSe (≈ 10 nm). They consist of 140 periods of the SL with a wider CdSe/ZnSe (3 nm) QW inserted after first fifty periods. Nominal thicknesses of CdSe (L_w) and ZnS_xSe_{1-x} (L_b) in the SLs are in the ranges 1.3–1.5 and 4–5 monolayers (ML), respectively, while the CdSe nominal thickness (L_{EQW}) in the extended QW is ≈ 2.8 ML, which implies formation of self-assembled CdSe quantum dots [5]. Main parameters of the fabricated structures are given in Table.

TABLE

Parameters of three structures with a CdSe/ZnS_xSe_{1-x} SL and a CdSe enlarged QW.

	x [%]	L_b [ML]	L_w [ML]	L_{EQW} [ML]
1	35–40	4	1.3	2.8
2	30	5	1.5	3.2
3	35-40	5	1.5	2.95

*corresponding author; e-mail: Evropeitsev@beam.ioffe.ru

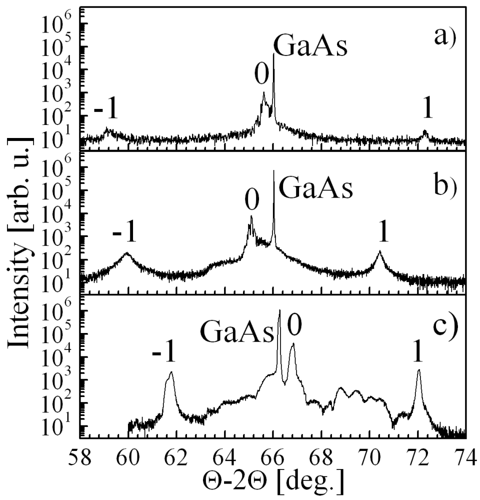

Fig. 1. XRD θ-2θ scans of the structures 1 — (a), 2 — (b) and 3 — (c) around the GaAs (004) diffraction reflex. The SL's satellites are labeled as "–1", "0", "1".

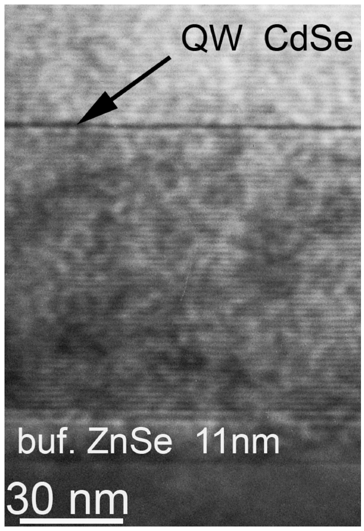

Fig. 2. TEM image of the cross-section of the 1st structure.

The lattice mismatch of the SL as a whole and the SL period are obtained by X-ray diffraction (XRD) θ-2θ scans, measured using a Cu K_α line (Fig. 1). One of the structures is studied by transmission electron microscopy (TEM). The temperature dependences of PL are registered with excitation by the emission of a halogen tungsten lamp dispersed by a monochromator. The PL spectra, measured at 77 K and 300 K, are detected with the excitation by a 404 nm laser line. The PL is dispersed by a spectrometer Acton 2500 and collected by a cooled CCD camera.

3. Results and discussion

The XRD θ-2θ scans of all three structures are presented in Fig. 1. The scans allow one to determine the period of each SL (from the angular distance between SL's satellites) and the average lattice parameter perpendicular to the SL layers planes $a_{\perp,av}$ (from the "zero" satellite peak position). The calculated SL periods equal 16, 20 and 20.6 Å for the structures 1–3, respectively; they are in a good agreement with the nominal periods of 15, 19 and 19 Å, defined by the structures design. The average lattice parameters are 5.686, 5.727 and 5.593 Å for 1–3 structures that correspond to lateral compressive strain in the SL of the 1st and 2nd structures and tensile strain for the 3rd structure. A TEM image of the cross-section of the 1st structure displays well resolved layers of the SL and enlarged QW. The SL period defined by TEM is 16 Å (Fig. 2). More detailed TEM studies revealed a negligibly small density of extended defects in this structure.

PL spectra of the structures, measured at 77 and 300 K, are presented in Fig. 3. All three structures demonstrate bright PL indicating perfect crystal quality. The efficiency of the carrier transport across the SL is estimated by measuring the relation $I^{\mathrm{EQW}}/I^{\mathrm{SL}}$, where I^{EQW} and I^{SL} are integral intensities of PL from enlarged QW and from SL, respectively, measured with an excitation energy above the SL absorption edge. PL intensities I^{EQW} and I^{SL} are of the same order of magnitude at 77 K (Fig. 3a), whereas I^{SL} values are considerably smaller than I^{EQW} at room temperature (Fig. 3b) that can be explained by the increase of the vertical transport efficiency due to temperature induced activation of the carriers localized within the SL.

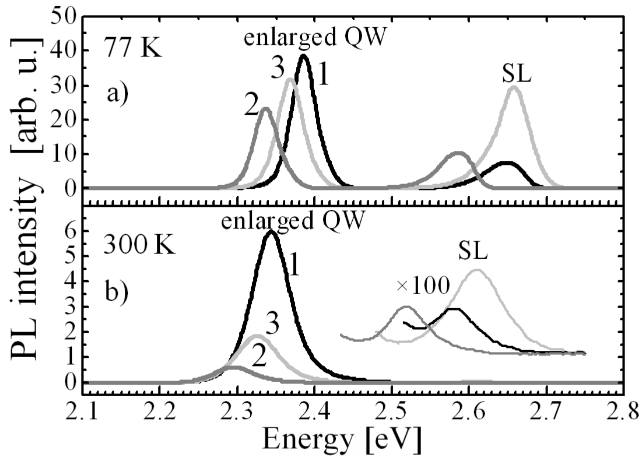

Fig. 3. PL spectra of three structures "1", "2", and "1" measured at 77 K (a) and 300 K (b). PL spectra from the SL measured at 300 K are multiplied by 100 and shifted up for clarity.

This interpretation is confirmed by temperature dependences of PL, measured for the 1st and 2nd structures with excitation by light with the photon energy either above the SL absorption edge or between the absorption edges of the SL and the enlarged QW. The spectral position (E_{peak}), and spectral width (FWHM) (Fig. 4), as well as the integral intensity (Fig. 5) of the PL lines from the SL show a weak temperature dependence at the lowest temperatures (< 20 K) that corresponds to the emission due to localized excitons in the SL. Above 20 K, the PL line from the SL in both structures shows a non-monotonous temperature dependence of the Stokes shift and the line spectral width with characteristic features observed at 70 K and 83 K, respectively. Such features are typically related to a carrier mobility increase as a result of delocalization processes [6]. Consequently, the exponential decrease of the PL intensity from the SL at temperatures above 20 K can be attributed to enhancement of the vertical transport of carriers through the SL.

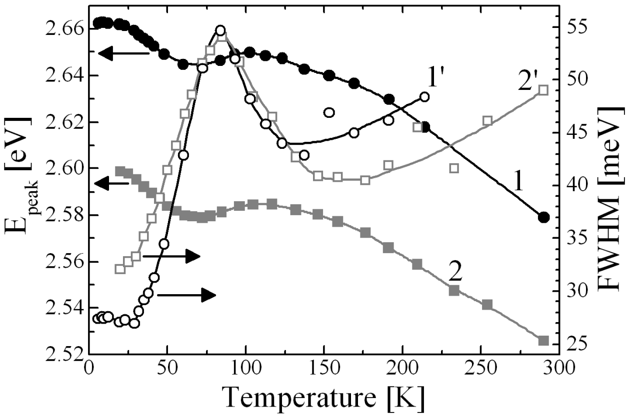

Fig. 4. Temperature dependence of the position and FWHM of the PL line detected from the enlarged QW or SL in the 1st structure (1, 1') and 2nd structure (2, 2').

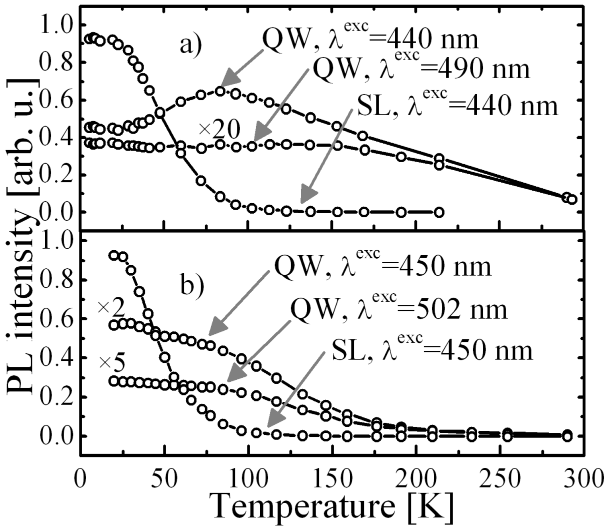

Fig. 5. Temperature dependence of integral intensity of the PL line detected from the enlarged QW and SL in the 1st structure (a) and 2nd structure (b). The wavelength of excitation is denoted by λ^{exc}.

The non-monotonous temperature dependence of the PL intensity from the enlarged QW in the 1st structure takes place only with excitation energy above the SL absorption edge that clearly demonstrates the increase of the vertical transport efficiency in the SL with temperature. The temperature dependences of the peak energy and FWHM of the PL line from the enlarged QW (not shown) are very similar for both structures and have features, mentioned above for the SL, but with characteristic temperatures 115–120 K (E_{peak}) and 140–145 K (FWHM). Consequently, the decrease of I^{EQW} ($E^{exc} < E_g^{SL}$) for the 1st structure at temperatures above 150 K can be ascribed to the carriers delocalization in the enlarged QW. Unlike the first structure, the decrease of I^{EQW} ($E^{exc} < E_g^{SL}$) for the 2nd one starts at temperatures less than 150 K, that can be explained by elevated nonradiative recombination resulting from the larger lattice mismatch of the 2nd structure (Fig. 1).

4. Conclusions

In this work we have fabricated by MBE the alternately-strained $ZnS_xSe_{1-x}/CdSe$ short period superlattices with the effective band-gap 2.52, 2.58, and 2.61 eV and thickness ≈ 300 nm on GaAs substrate. The SLs are designed to obtain efficient vertical transport at room temperature while maintaining lattice-matched conditions. TEM, XRD and photoluminescence investigations of the structures revealed negligibly small density of misfit dislocations. Photoluminescence study of carrier vertical transport in the SLs containing enlarged QW confirms the Bloch-type transport of carriers at the temperatures above 100 K. Adjustable band-gap energy, defect-free growth of the SL on the GaAs substrate and high efficiency of vertical transport make it possible to utilize such SLs as a material of a wide band-gap cascade of a multi-junction solar cell comprising both III–V and II–VI materials.

Acknowledgments

This work is financially supported by the Ministry of Education and Science of Russian Federation, project #14.604.21.0008 from 17.06.2014 with the applied research unique identifier RFMEFI60414X0008. The studies were partly carried out in Joint Research Center "Material science and characterization in advanced technology" under financial support of the Ministry of Education and Science of the Russian Federation.

References

[1] Y.H. Zhang, S.N. Wu, D. Ding, S.Q. Yu, S.R. Johnson, *Proc. 33rd IEEE Photovoltaic Specialists Conference, San Diego (CA, USA)*, IEEE, 2008, p. 62.

[2] M.A. Haase, J. Qiu, J.M. DePuydt, H. Cheng, *Appl. Phys. Lett.* **59**, 1272 (1991).

[3] T.V. Shubina, S.V. Ivanov, A.A. Toropov, G.N. Aliev, M.G. Tkatchman, S.V. Sorokin, N.D. Il'inskaya, P.S. Kop'ev, *J. Cryst. Growth* **184/185**, 596 (1998).

[4] A. Chomette, B. Deveaud, J.Y. Emery, A. Regreny, B. Lambert, *Solid State Commun.* **54**, 75 (1985).

[5] S.V. Ivanov, A.A. Toropov, T.V. Shubina, S.V. Sorokin, A.V. Lebedev, I.V. Sedova, P.S. Kop'ev, G.R. Pozina, J.P. Bergman, B. Monemar, *J. Appl. Phys.* **83**, 3168 (1998).

[6] S.D. Baranovskii, R. Eichmann, P. Thomas, *Phys. Rev. B* **58**, 13081 (1998).